Supporting Information Appendix

CryoEM Structure and Mechanism of the Membrane-Associated Electron Bifurcating Flavoprotein Fix/EtfABCX

Feng et al.

This document contains:

Supplementary Tables S1 - 3

Supplementary Figures S1 - 10

Supplementary Movie S1

Supplementary Table S1. Cryo-EM data collection, refinement, and validation statistics for the *T. maritima* EtfABCX complex

	EtfABCX (EMD-22973, PDB 7KOE)
Data collection and processing	
Microscope	Titan Krios
Voltage (kV)	300
Electron exposure ($e^{-}Å^{-2}$)	80
Defocus range (–μm)	1.0 to 2.0
Pixel size (Å)	1.029
Symmetry imposed	C2
Initial particle images (no.)	2,471,763
Final particle images (no.)	285,377
Map resolution (Å)	2.9
FSC threshold	0.143
Map resolution range (Å)	247.0-2.9
Refinement	
Map sharpening B factor ($Å^2$)	87
Model composition	
Non-hydrogen atoms	18,348
Protein residues	2,296
R.m.s. deviations	
Bond lengths (Å)	0.01
Bond angles (°)	1.3
Validation	
MolProbity score	2.25
Clashscore	10.9
Poor rotamers (%)	2.18
Ramachandran plot	
Favored (%)	93.2
Allowed (%)	6.71
Outliers (%)	0.1

Supplementary Table S2. Primers for plasmid and strain construction for *Tma* EtfABCX expression in *P. furiosus* (strain MW369)

Primer	Sequence (5'-3')	Description
GL442	GATTATTGGGAGGTGGAGAAAAATGGCACATCA CCACCATCACCACCACCATCACGCTAATGTGGT TGTCTGTATCAAAC	pGL093 Gibson assembly (EtfABCX) with 9x his-tag
GL443	TCACCCGAATTTGTAGAGC	pGL093 Gibson assembly (EtfABCX)
GL444	GCTCTACAAATTCGGGTGAAATCTTTTTTAGCAC TTTTGGCG	pGL093 Gibson assembly (plasmid backbone)
SP2.055	TTTTCTCCACCTCCCAATAATC	pGL093 Gibson assembly (plasmid backbone)
SP.129	GCCTCCGACTAACGAAAATCC	pGL093 PCR confirmation (sequencing)
SP.130	GCTAAATACGGAAGGATCTGAGG	pGL093 PCR confirmation, (sequencing)
GL209	GATCTAAAGCTGGCAGACATC	pGL093 PCR confirmation, (sequencing)
GL445	TTGAGCGACAGGACGTTC	Sequencing, qPCR (EtfA)
GL446	AGCAAGACCAGGTCCCAC	Sequencing, qPCR (EtfA)
GL447	GGATCACAGACCGCAGATG	Sequencing. qPCR (EtfB)
GL448	GTCTGAAGCGGTATGGTTTCC	Sequencing, qPCR (EtfB)
GL449	GGTGTGAATCCCATCCTCAC	Sequencing, qPCR (EtfC)
GL450	CGTTGCTCCATCGTTTCC	Sequencing, qPCR (EtfC)
GL451	GAACAGATACAGAACGGATGAGG	Sequencing, qPCR (EtfX)
GL452	CGAATTTCACCTCCATTCCACTC	Sequencing, qPCR (EtfX)
SP2.105	AAGTTGTGTGGAGAGCTTTCG	*P. furiosus* Genome Region 5 (PCR confirmation)
SP2.106	CTGGACTCCTTCTAACGCAG	*P. furiosus* Genome Region 5 (PCR confirmation)

Supplementary Table S3. Abbreviations used in the text.

EtfABCX	Electron transferring flavoprotein-menaquinone oxidoreductase ABCX (tetrameric, bifurcating)
EtfAB	Electron transfer flavoprotein (dimeric subcomplex, bifurcating)
ETF	Electron transfer flavoprotein (canonical)
FBEB	Flavin-based electron bifurcation
FixABCX	Electron transferring flavoprotein-menaquinone oxidoreductase ABCX complex found in some N_2-fixing microbes (tetrameric, bifurcating)
Q/QH_2	Quinone/quinol
E	Redox potential
E°'	Standard redox potential at pH 7
E_m	Midpoint potential
HydABC	Trimeric [FeFe]-hydrogenase (bifurcating)
HdrA	Heterodisulfide reductase subunit A
Nfn	NADH-dependent ferredoxin NADPH oxidoreductase (bifurcating)
EtfAB-Bcd	Electron transferring flavoprotein/Butyryl-CoA dehydrogenase (bifurcating)
CarCDE	Caffeyl-CoA reductase (bifurcating)
MvhADG-HdrABC	Hydrogenase CoB-CoM heterodisulfide reductase (bifurcating)
MQ	Menaquinone
BF-FAD	Bifurcating FAD
ET-FAD	Electron transfer FAD
QR-FAD	Quinone reductase FAD
CT	Charge transfer complex
Pae	*Pyrobaculum aerophilum*
Tma	*Thermotoga maritima*
Fd	Ferredoxin
LDAO	Lauryldimethylamine N-oxide
DDM	n-Dodecyl-β-D-maltoside
ETF-QO	ETF ubiquinone oxidoreductase
RMSD	root-mean-square deviation of atomic positions
HH	Horizontal helix
mV	Millivolt
OX	Oxidized
ASQ	Anionic semiquinone
NSQ	Neutral semiquinone
HQ	Hydroquinone

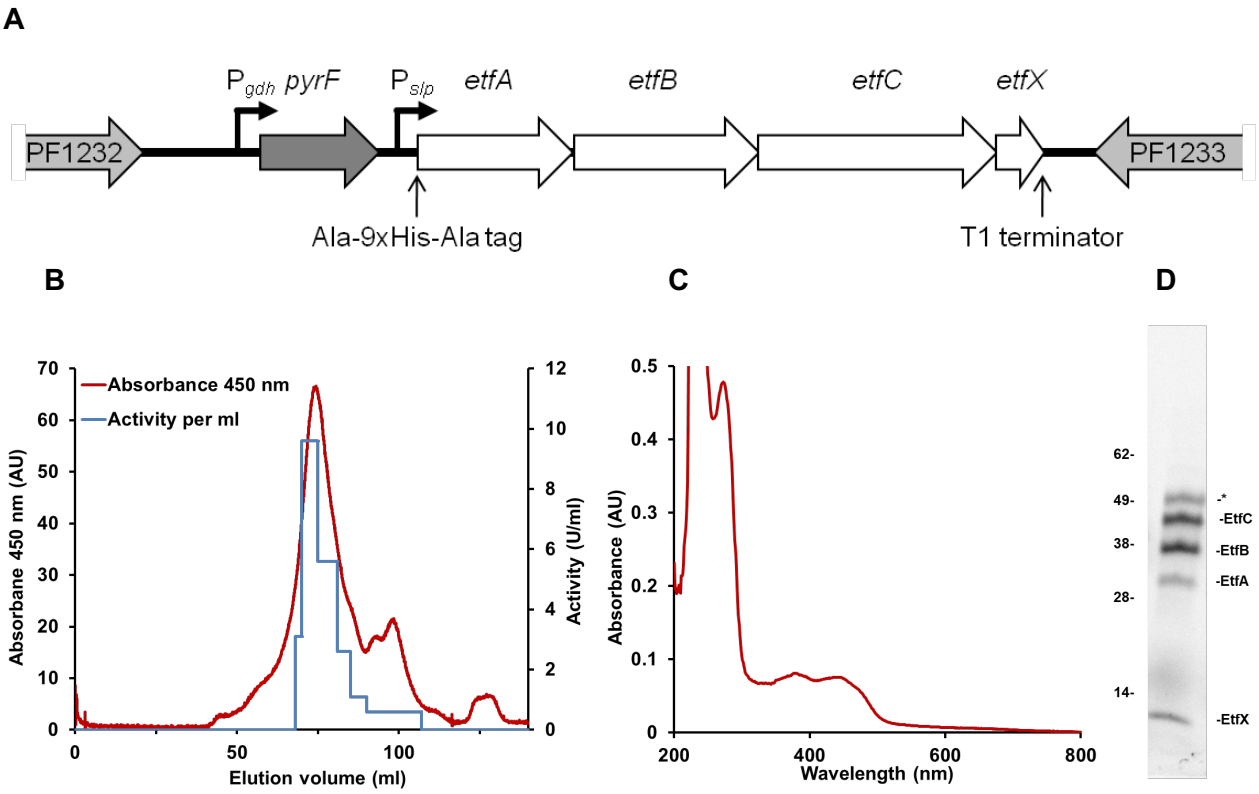

Supplementary Figure S1. A. Arrangement of the *T. maritima* EtfABCX expression cassette (PslpetfABCX) inserted into the *P. furiosus* genome. **B.** Size exclusion column (Superdex S200 column; 16/60; Cytiva) elution profile for Tma EtfACX. Fractions were analyzed for flavin content (A_{450}, red trace) and NADH oxidation activity (discontinuous blue trace). **C.** UV/vis spectrum of Tma EtfABCX. **D.** Gel electrophoresis of the purified EtfABCX sample used structure determination (*indicates and unknown contaminating protein).

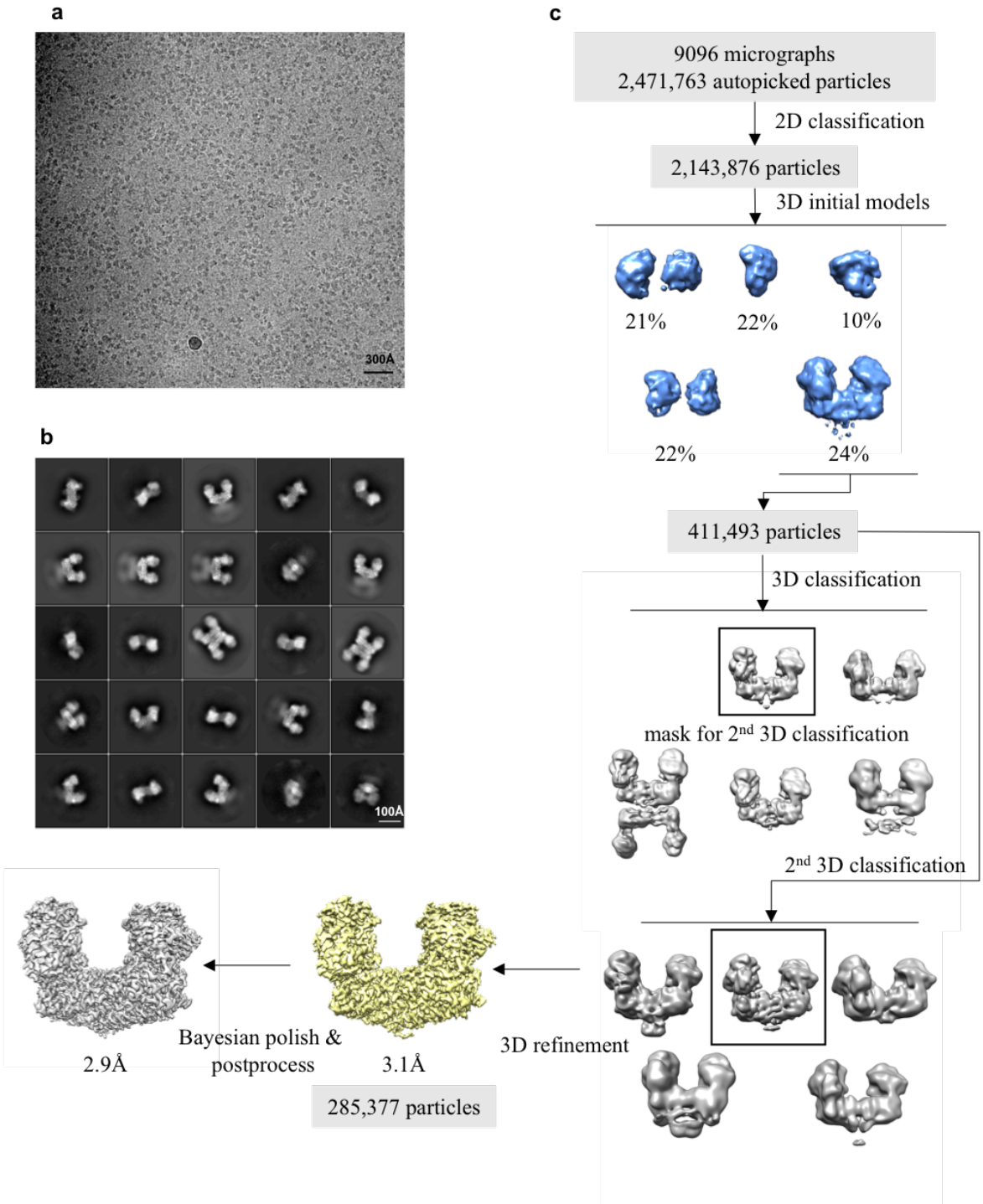

Supplementary Figure S2. Cryo-EM of the Tma EtfABCX complex. (**a**) A typical electron micrograph. (**b**) 2D class averages demonstrating a heterogeneous population of particles. (**c**) Flow chart of 2D and 3D classifications, and 3D refinement and reconstruction.

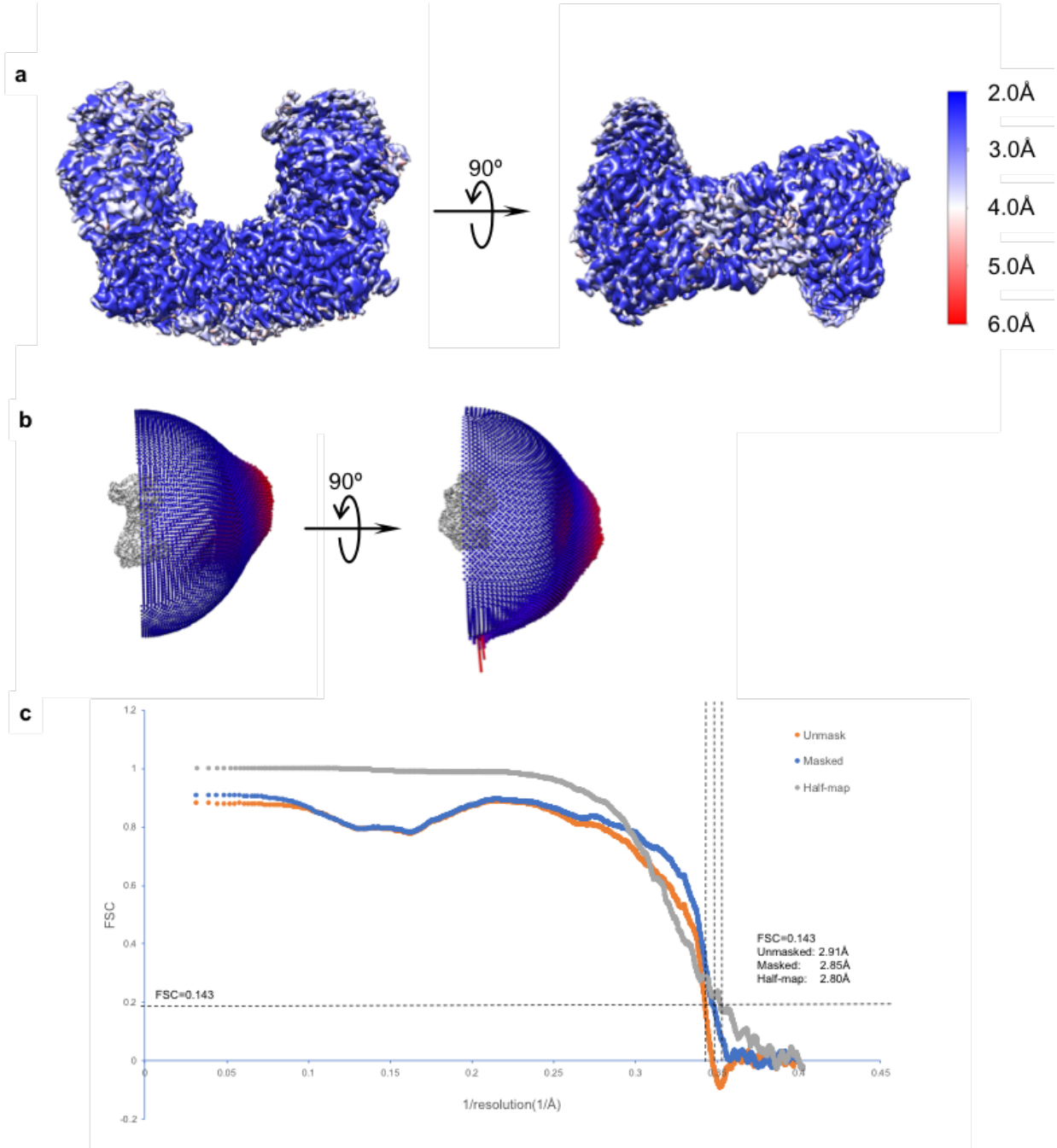

Supplementary Figure S3. Analysis of the electron density map. Local resolution (**a**), angular distribution of the raw particle images (**b**) and Fourier shell correlation (FSC) curve (**c**) for masked and unmasked 3D map of the EtfABCX complex.

Detergent	"X" shaped particles	"U" shaped particles
		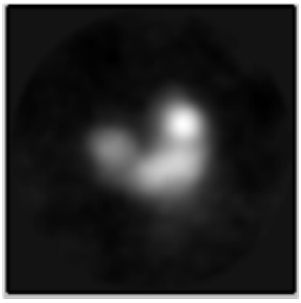
No detergent	8.4%	5.1%
0.02% DDM	0.0%	13.1%
0.01% LDAO	4.3%	8.0%

Supplementary Figure S4. Detergent breaks the in vitro hydrophobic interface between two (EtcABCX)$_2$ octamers. (A) A typical view of the X-shaped particles comprised of two copies of (EtfABCX)$_2$ docked end-to-end via their respective membrane-embedding hydrophobic surface. **(B)** A typical side view of the U-shaped (EtfABCX)$_2$ complex. The population of two arrangement can be told by comparing the size of 2D classes. After adding detergents, the distribution of the particles strongly favored octamer rather than 16-mer assembly.

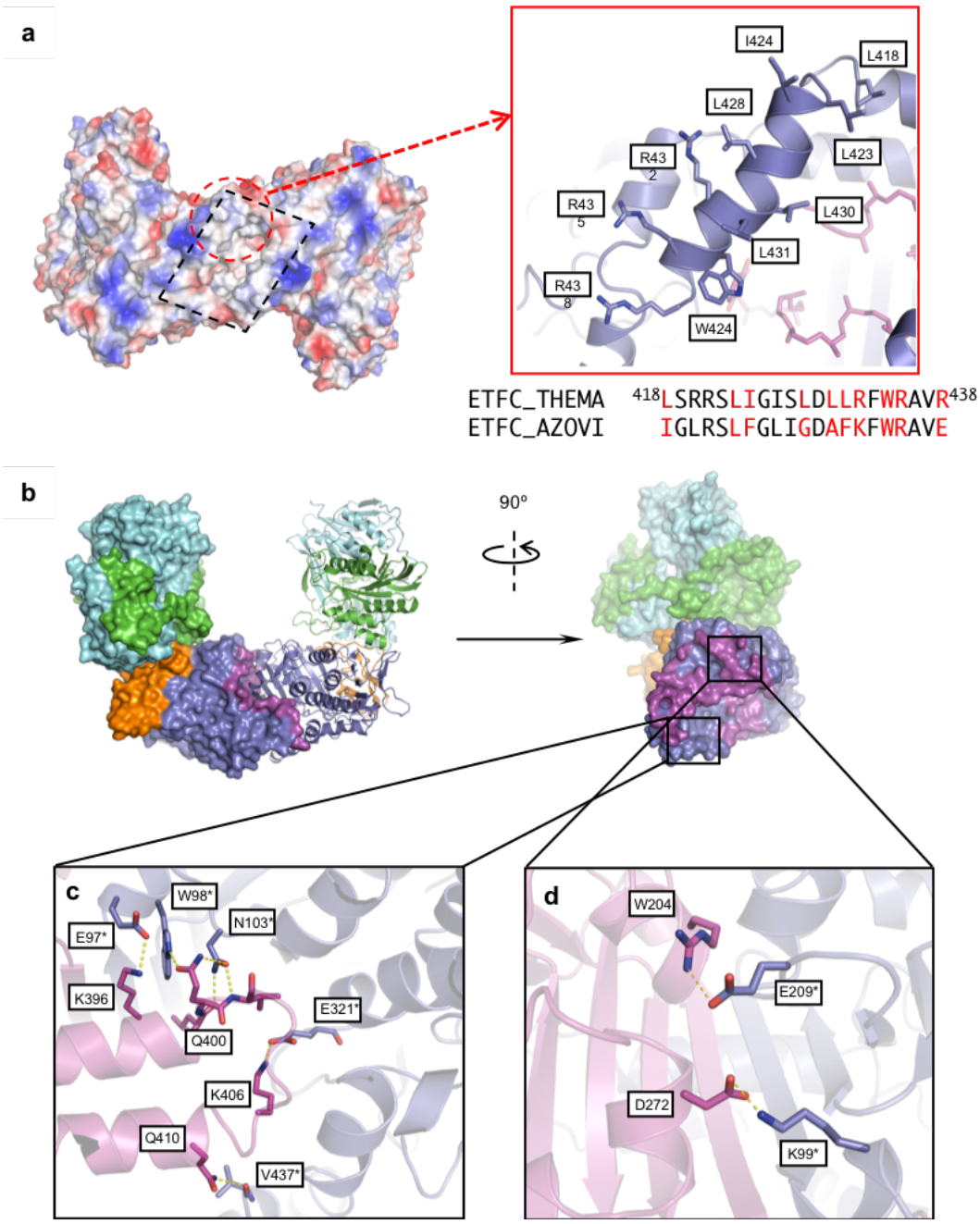

Supplementary Figure S5. The dimerization interface in the EtfC dimer. (**a**) A bottom view of the surface charge plot of EtfABCX. The central region may sink into the lipid bilayer as it contains a hydrophobic patch that is surrounded by positively charged residues. The positive residues may bind the negatively charged head group of the phospholipids. (**b**) The EtfC-EtfC dimer interface. Left: front side view of the EtfABCX super dimer. Right: right side view with the front protomer 2 removed to show the dimer interface in EtfC. (**c**) The C-terminal helix-turn-helix inserts into the groove of a symmetry-related protomer, forming hydrophobic and charge interactions. (**d**) Inter-molecular β-sheet (background) and salt bridges of two short α-helix form the extensive dimer interface. Amino acid number with an asterisk refers to residue from the symmetry-related protomer.

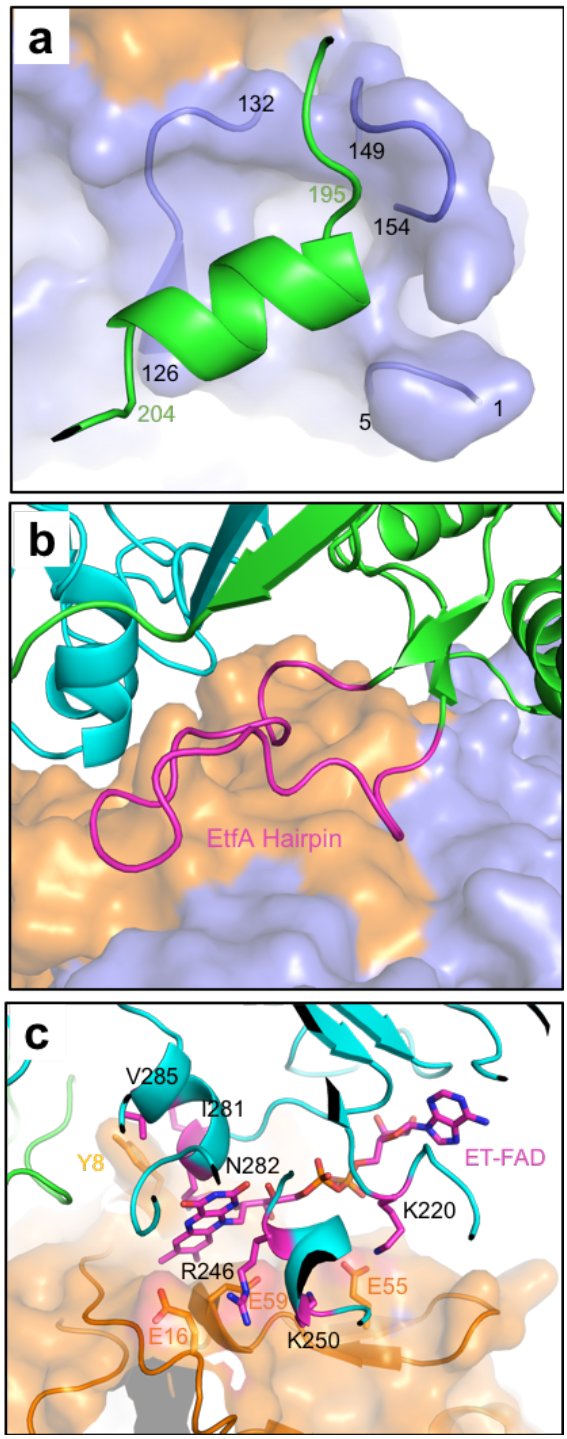

Supplementary Figure S6. Three Interfaces between EtfAB and EtfCX. EtfA has two interfaces with EtfC (**a, b**) and EtfB has one interface with EtfX (**c**). The interface between EtfB and EtfX also form the binding pocket for ET-FAD.

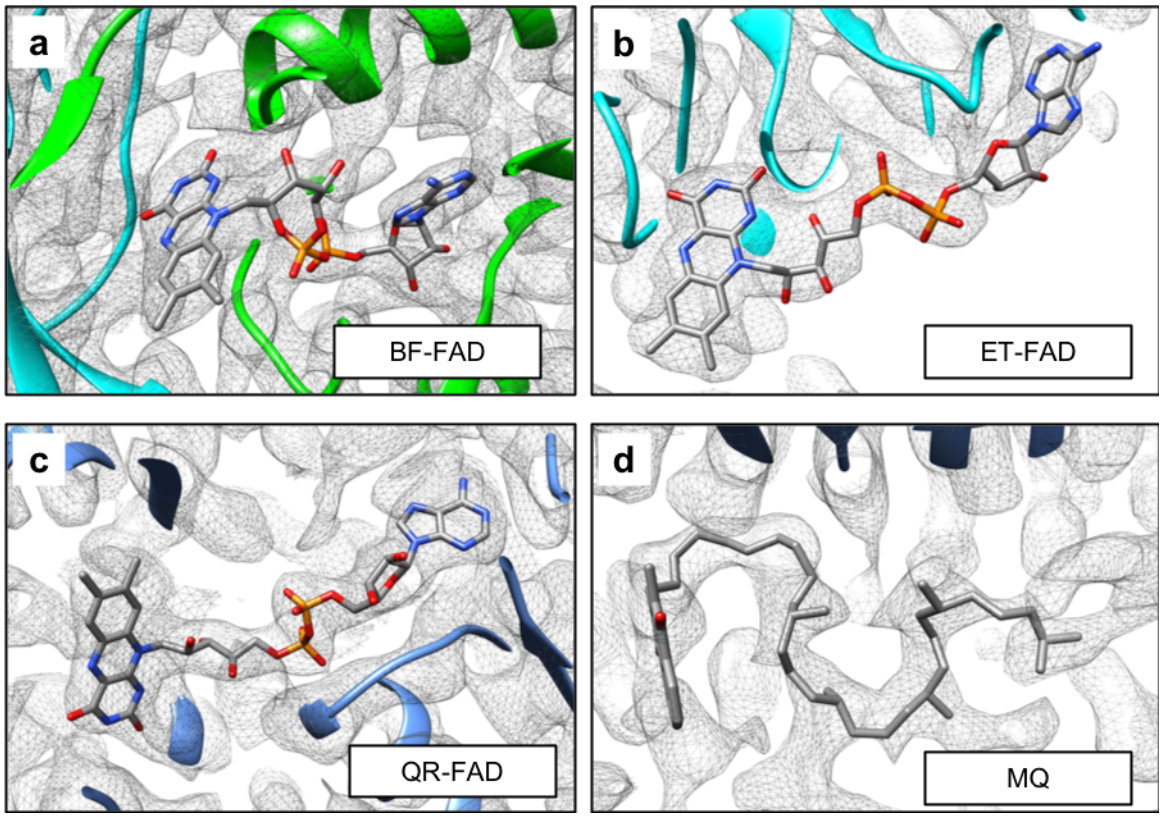

Supplementary Figure S7. The electron densities of the three bound FAD molecules and one MQ in cryo-EM map of the EtfABCX. The electron densities surrounding BF-FAD (**a**), ET-FAD (**b**), QR-FAD (**c**), and MQ (**d**) are surface rendered and shown in grey meshes.

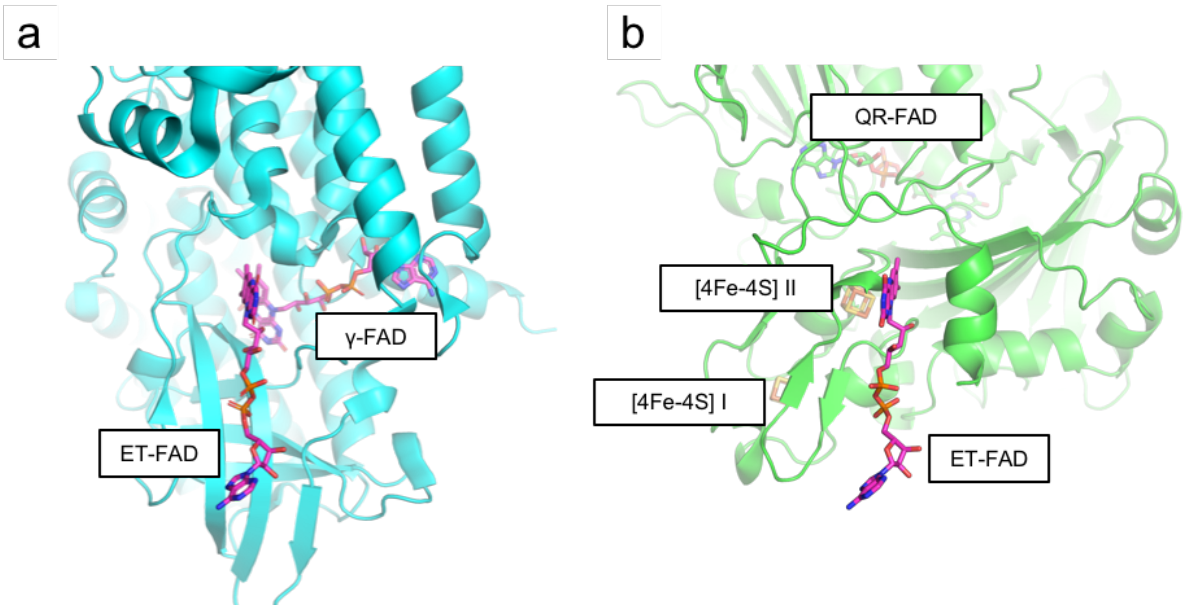

Supplementary Figure S8. Coupling with the ET-FAD in Bcd-EtfAB and EtfABCX. Bcd (PDB ID 6FAH) and EtfCX are colored cyan and green, respectively. The two complexes are superimposed by aligning their respective Domain II. Domain II is hidden for simplicity. FADs are shown as magenta sticks.

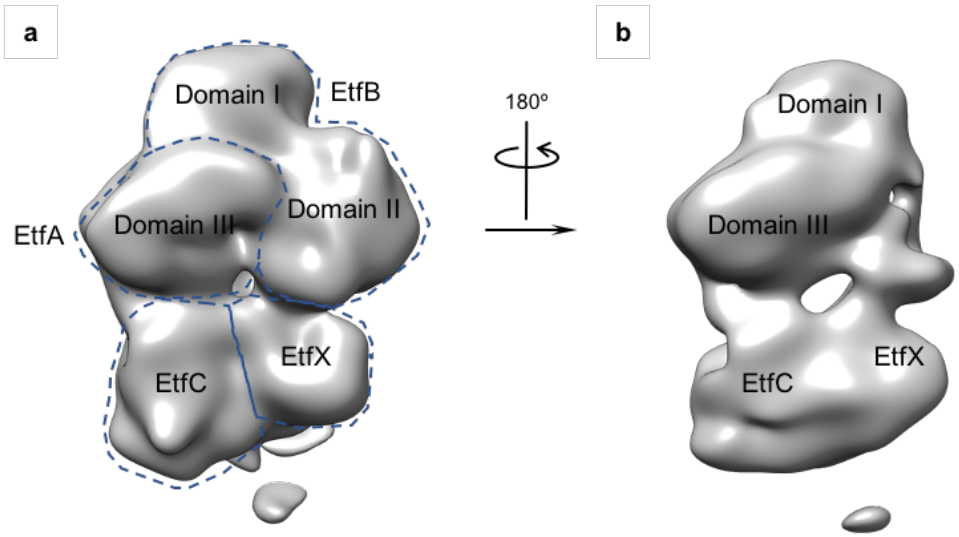

Supplementary Figure S9. Comparison of 3D maps of two monomeric EtfABCX particles indicates the domain II flexibility. (**a**) EtfABCX particles with defined density for domain II. (**b**) EtfABCX particles with the domain II density largely missing.

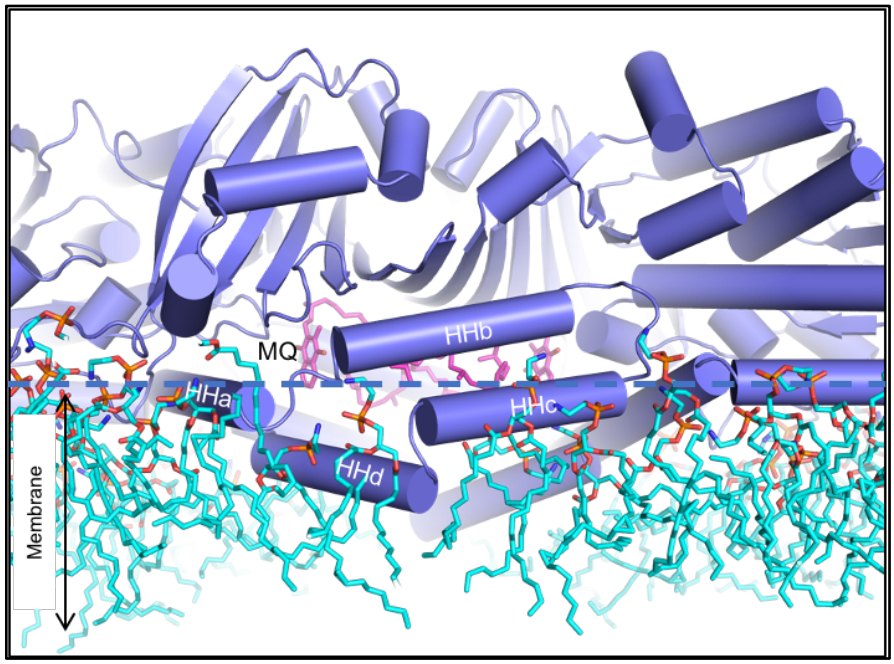

Supplementary Figure S10. MD simulation of the phospholipid binding region on the lower surface of EtfC comprised of the C-terminal four helices HHa-HHd. In this side view, the negatively charged head groups of lipids bind the positively charged resides and the lipid tails interact with the hydrophobic residues of the two HHd helices.

Supplementary Movie S1. A comparison of the location and orientation of EtfAB domain II in different states. The models were generated using previously solved EtfAB under different states as templates. The movement between different models were generated using "morph" command in ChimeraX [1], which is also used to generate the movie.

1 Goddard, T. D. *et al.* UCSF ChimeraX: Meeting modern challenges in visualization and analysis. *Protein science : a publication of the Protein Society* **27**, 14-25, doi:10.1002/pro.3235 (2018).